Giant quantum freezing of nanojunctions mediated by the environment

A. Glatz,[1] N. M. Chtchelkatchev,[2,3,*] I. S. Beloborodov,[4] and V. Vinokur[1]

[1]*Materials Science Division, Argonne National Laboratory, Argonne, Illinois 60439, USA*

[2]*Institute for High Pressure Physics, Russian Academy of Science, Troitsk 142190, Russia*

[3]*Department of Theoretical Physics, Moscow Institute of Physics and Technology, 141700 Moscow, Russia*

[4]*Department of Physics and Astronomy, California State University Northridge, Northridge, California 91330, USA*

(Received 16 November 2011; published 1 December 2011)

We investigate the quantum heat exchange between a nanojunction and a many-body or electromagnetic environment far from equilibrium. It is shown that the two-temperature energy emission-absorption mechanism gives rise to a giant heat flow between the junction and the environment. We obtain analytical results for the heat flow in an idealized high-impedance environment, perform numerical calculations for the general case of interacting electrons, and discuss giant freezing and heating effects in the junction under typical experimental conditions.

DOI: 10.1103/PhysRevB.84.235101 PACS number(s): 05.70.Ln, 72.15.Jf, 73.63.−b, 85.80.Fi

I. INTRODUCTION

Electron transport in the presence of an electric field is always accompanied by heating of the charge carriers. This effect is especially pronounced in electronic devices, where overheating leads to instabilities in the current-voltage characteristics.[1,2] This defines the urgent task of studying far-from-equilibrium heating of charge carriers.

In this paper we study the heat flow between tunneling electrons and an environment in nanojunctions using a nonperturbative technique based on a quantum kinetic equation. We show that a regime exists in which the interaction with the environment leads to an effective ("giant") environment cooling of the junction.

At high electron temperatures phonons play the role of the cooling agent. At low temperatures the direct energy transfer to the phonon bath becomes inefficient and the relaxation is dominated by energy exchange between tunneling electrons and an electromagnetic environment and/or environment of many-body excitations in the electrodes.[3] In both cases, cooling follows the two-temperature emission-absorption mechanism:[1,3] the emission of environment modes with a temperature equal to that of the tunneling charge carriers, T_e, and the absorption of environment excitations having the temperature of the environment, $T_{\rm env}$. Moreover, not only temperatures, but also the distributions of emitted and absorbed environment modes, may be different in the far from equilibrium regime.

The coupling between the tunneling electrons and the environment has a dispersion characterized by the "cut-off" frequency $\omega_{\max}$. For example, $\omega_{\max} = E_c$ for a high-impedance environment, with E_c being the charging energy of the tunnel junction; $\omega_{\max} = 1/\sqrt{LC}$ for an environment represented by an L-C circuit; and $\omega_{\max} = 1/R_T C$ for an ohmic environment, with R_T and C being the ohmic resistance[4,5] and capacitance of the tunnel junction, respectively.[6] We are interested in the regime where $T_e, T_{\rm env} > \omega_{\max}$. In this case the large number of environment modes, $\mathcal{N} \sim \ln[\omega_{\max}\tau_e(T_e)]\max\{T_e, T_{\rm env}\}/\omega_{\max} \gg 1$ (τ_e is the energy relaxation rate), participate in the heat exchange between the environment and tunneling electrons in the nanojunction. At low electron temperatures, when the environment has an electromagnetic or many-body origin, this regime is easy to reach.[6,7] We show that in general the heat flux acquires the large factor $\mathcal{N} \gg 1$ in all orders in electron-environment interactions increasing the efficiency of the heat exchange. Using the Landauer scattering theory[8] we express the density matrix as the direct product of the density matrices for emitted and absorbed environment excitations; this is a typical case for a two-temperature emission-absorption mechanism far from equilibrium. The validity of the Landauer approach implies that the effective energy relaxation length of the environment modes is larger than the size of the nanostructure.

In our consideration a bath (phonons) is absent. Therefore our approach is valid when the interaction time between electrons and environment is much smaller than the one between environmet and bath, which is the case at not very high temperatures where the number of phonons is small.

II. MODEL

The rate of heat flow between the tunnel junction and the environment is given by (see Appendix A and Ref. 7)

$$\dot{Q} = \int_0^\infty \varepsilon\{n_\varepsilon P(\varepsilon) - [1+n_\varepsilon]P(-\varepsilon)\}p(\varepsilon)d\varepsilon, \qquad (1)$$

where $P(\pm\varepsilon)$ is the probability density for the tunneling charge carrier to lose (gain) the energy ε to (from) the environment. The distribution function n_ε in Eq. (1) can be interpreted as the distribution function of electron-hole pairs that appear at the junction interface just after the tunneling process: the hole in the source lead and the electron in the drain [Fig. 2(a)]. The effective temperature of "tunneling electrons" T_e should be identified with $\lim_{\varepsilon\to 0} n_\varepsilon$. If the distribution functions at the electrodes are Fermi functions with equal temperatures T, then $n_\varepsilon = \{(\varepsilon - V)N_B(\varepsilon - V, T) + (\varepsilon + V)N_B(\varepsilon + V, T)\}/2\varepsilon$, with $N_B(\varepsilon \pm V, T)$ being the equilibrium Bose distribution function. For this case, $T_e = \frac{V}{2}\coth\frac{V}{2T}$. At low applied voltages, $V \ll T$, and $T_e \approx T$. In the opposite case, $V \gg T_e$, we obtain $T_e \approx V/2$. The function $p(\varepsilon)$ in Eq. (1) is the weight function for a junction between two normal metals (Fig. 1) and can be calculated for any choice of the electron distribution function in the leads, resulting in $p(\varepsilon) = 4\varepsilon/R_T$.

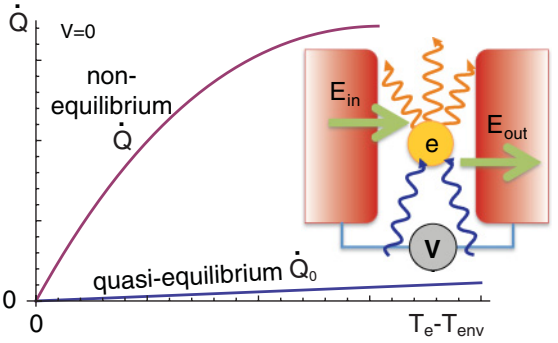

FIG. 1. (Color online) Illustration of the nonequilibrium heating effects in a nanojunction. Electrons traversing the junction absorb external photons (incident wavy lines) and emit them, leading to heating of the contact. Plots show the *giant* heating effect, $\dot{Q}$, as a function of the difference of electron and environment temperatures ($V = 0$) compared to the "quasiequilibrium" approximation, where the radiation density matrix is equilibrium, $\dot{Q}_0$. The full nonequilibrium analysis gives a heating effect that is at least 1 order of magnitude more pronounced than for the latter case: $\max(\dot{Q}/\dot{Q}_0) \sim \mathcal{N} > 10$.

III. HEAT FLOW

To calculate $\dot{Q}$, one has to specify the probability density, which can be written in the form $P(\varepsilon) = \int_{-\infty}^{\infty} dt \exp[J(t) + i\varepsilon t]$, where the function $\exp[J(t)]$ reflects the fact that tunneling electrons acquire random phases due to interaction with the Bosonic environment. The equilibrium situation where the distribution function of the environment modes is the Bose distribution was discussed in Ref. 6. In the general far-from-equilibrium situation, the function $J(t)$ can be written as[3]

$$J(t)/2 = \int_{[\tau_e(T_e)]^{-1}}^{\infty} \frac{d\omega}{\omega}\rho(\omega) \times \left[N_\omega^{(\mathrm{in})} e^{i\omega t} + \left(1 + N_\omega^{(\mathrm{out})}\right)e^{-i\omega t} - B_\omega\right], \quad (2)$$

where the terms proportional to $N_\omega^{(\mathrm{in})}$ and $1 + N_\omega^{(\mathrm{out})}$ correspond to the absorbed and emitted environment excitations, respectively, and $B_\omega = 1 + N_\omega^{(\mathrm{out})} + N_\omega^{(\mathrm{in})}$. At equilibrium, N_ω reduces to the Bose function and the functional $P(\omega)$ recovers the result in Ref. 6. The energy relaxation time τ_e in the expression for $J(t)$ determines the low-energy cutoff, since the electrons start to equilibrate on larger time scales, i.e., the nonequilibrium description does not hold any more. The spectral function $\rho(\omega)$ is the probability of the electron-environment interaction and characterizes the particular system under consideration.

According to scattering theory, modes coming from one "reservoir" into the other have the temperature of the "reservoir" of their origin.[8] Then the second quantization operators $c_\alpha^{(\mathrm{in/out})}$ of the emitted (absorbed) environment mode α enter the density matrix

$$\wp = e^{-\sum_\alpha (c_\alpha^{(\mathrm{in})})^\dagger c_\alpha^{(\mathrm{in})}/T_{\mathrm{in}}} \times e^{-\sum_\alpha (c_\alpha^{(\mathrm{out})})^\dagger c_\alpha^{(\mathrm{out})}/T_{\mathrm{out}}}, \quad (3)$$

where $T_{\mathrm{in}} = T_{\mathrm{env}}$ and $T_{\mathrm{out}} = T_e$. Thus $N_\omega^{(\mathrm{in})} = \langle (c_\omega^{(\mathrm{in})})^\dagger c_\omega^{(\mathrm{in})}\rangle = N_B(\omega, T_{\mathrm{env}})$ and $N_\omega^{(\mathrm{out})} = N_B(\omega, T_e)$. The quasiequilibrium approximation mentioned above corresponds to the Gibbs distribution of the environment modes: $\wp_0 = \exp\{-\sum_\alpha c_\alpha^\dagger c_\alpha / T_{\mathrm{env}}\}$.

To estimate the magnitude of the heat flow $\dot{Q}$, we first expand the distribution function $P(\varepsilon)$ in Eq. (1), in the first order in $\rho(\varepsilon)$:

$$\dot{Q}^{(1)} = \frac{8}{R_T}\int_{\tau_e^{-1}}^{\infty} d\varepsilon\varepsilon\rho(\varepsilon)\left\{n_\varepsilon\left(1 + N_\varepsilon^{(\mathrm{out})}\right) - (1 + n_\varepsilon)N_\varepsilon^{(\mathrm{in})}\right\}. \quad (4)$$

This expression becomes 0 if $n_\varepsilon = N_\varepsilon^{(\mathrm{in})} = N_\varepsilon^{(\mathrm{out})}$. If the distribution functions are not equal to each other, we can expand $\dot{Q}^{(1)}$ with respect to their difference. We consider the case where the voltage bias at the nanojunction is 0 but the temperatures of electrons at the leads and those that comprise the environment are slightly different, $T_e = T + \delta T/2$ and $T_{\mathrm{env}} = T - \delta T/2$. Thus, $n_\varepsilon = n_\varepsilon(T + \delta T/2)$, $N_\varepsilon^{(\mathrm{in})} = n_\varepsilon(T - \delta T/2)$, and $N_\varepsilon^{(\mathrm{out})} = n_\varepsilon(T + \delta T/2)$, where n_ε is the Bose distribution function. Expanding $\dot{Q}^{(1)}$ in the first order in a small parameter $\delta T/T \ll 1$, we find

$$\dot{Q}_\theta^{(1)} \approx \delta T \frac{8}{R_T}\int_{\tau_e^{-1}}^{\infty} d\varepsilon\varepsilon\rho(\varepsilon)n_\varepsilon'(T)[1 + \theta n_\varepsilon(T)], \quad (5)$$

where $n_\varepsilon'(T) = dn_\varepsilon(T)/dT$. The index θ is 0 for the quasiequilibrium situation when the temperatures of emitted and absorbed environment excitations are equal and 1 for the nonequilibrium case (the index 1 is skipped throughout this paper). Since $n_\varepsilon(T)$ in Eq. (5) is always positive, the following inequality is valid: $|\dot{Q}_0^{(1)}| < |\dot{Q}^{(1)}|$, where $\dot{Q}_0^{(1)}$ and $\dot{Q}^{(1)}$ refer to the heat flux in the quasiequilibrium and in nonequilibrium cases, respectively. The interaction function $\rho(\varepsilon)$ in Eq. (5) quickly decays at energies higher than some characteristic frequency $\omega_{\max}$. For temperatures $T > \omega_{\max}$ we can approximate $n_\varepsilon(T) \approx T/\varepsilon \gg 1$ and find

$$\frac{|\dot{Q}^{(1)}|}{|\dot{Q}_0^{(1)}|} \approx \frac{\int_{\tau_e^{-1}}^{\infty} \frac{T\rho(\varepsilon)d\varepsilon}{\varepsilon}}{\int_{\tau_e^{-1}}^{\infty}\rho(\varepsilon)d\varepsilon} \approx \frac{T}{\omega_{\max}}\ln(\omega_{\max}\tau_e) \equiv \mathcal{N} \gg 1. \quad (6)$$

Remarkably, at higher orders with respect to $\rho(\varepsilon)$, the nonequilibrium heat flow $\dot{Q}$ differs from the equilibrium flow $\dot{Q}_0$ by the same factor. This result holds even for a finite electric current flowing through the junction. Thus, the heat flow between the junction and the environment appears much larger than what the quasiequilibrium estimates predict.

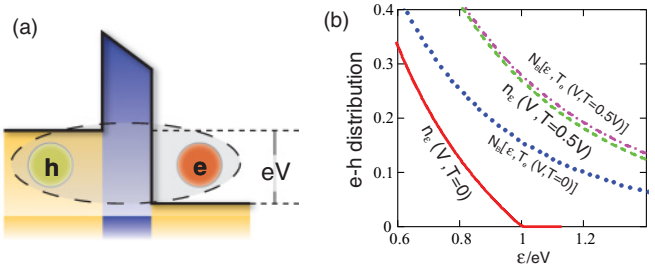

FIG. 2. (Color online) (a) Illustration of electron-hole pair generation in the tunnel junction, resulting in the distribution function n_ε [Eq. (1)] of these pairs (environment). (b) Comparison of the distribution functions for $T = 0$ in the leads and $T = V/2$.

IV. OHMIC APPROXIMATION

We now turn to the simplest case, an environment with a very high impedance compared to the quantum resistance, R_Q.

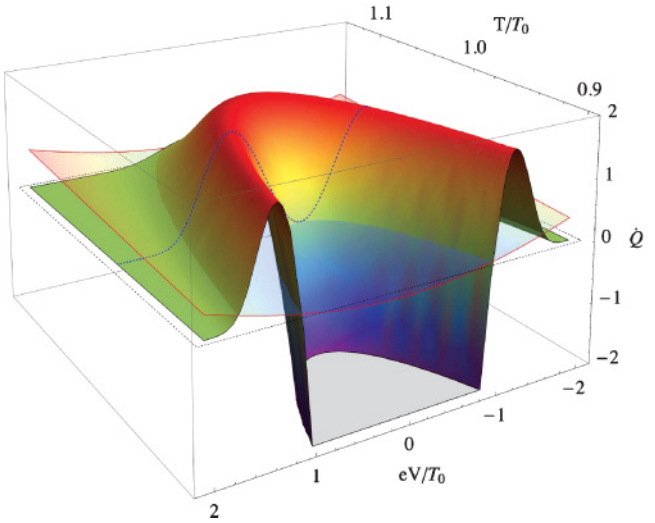

FIG. 3. (Color online) Typical heat exchange $\dot{Q}$ in Eq. (1) of the ohmic environment with the tunnel junction between two normal leads. $\dot{Q}(T_{\rm eff}, T, V)$ vs T/T_0 and voltages eV/T_0 (scaling factor $T_0 = 30\omega_{\rm max}$.). We used $\omega_{\rm max}/\omega_{\rm min} = 100$, $T_{\rm env}/T_0 = 1$, and $\rho(0) = 10$. $\dot{Q}$ is measured in units of $10^3\omega_{\rm max}^2/(e^2R_T)$.

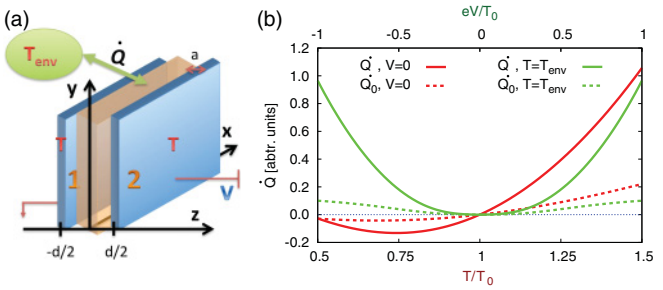

FIG. 4. (Color online) (a) Schematic presentation of the system: single contact junction, with contacts consisting of two thin plates, which are distance d apart. Their thickness a is much less than the extension in the x and y directions, such that they can be treated as two-dimensional contacts. The temperature of the contacts T is kept constant, while the environment temperature $T_{\rm env}$ can be different, which results in heat production or removal in the junction. (b) Heating of a tunnel junction taking into account dynamic Coulomb interactions for the zero bias case ($V = 0$) (red lines, lower x axis) and the voltage dependence for $T = T_e$ (green lines, upper x axis). The solid curves represent the quasiequilibrium curves and the dashed curves assume an equilibrium distribution for N_ω (temperature in units of $T_0 = 0.1E_{\rm th}$).

In this limit, tunneling electrons easily excite the environment modes. The spectral density $\rho(\omega)$ of these modes is sharply peaked at the zero frequency, $\omega = 0$. For the correlation function $J(t)$ the concentration of the environment modes at low frequencies implies that the expansion of $J(t)$ over t up to second order yields $J(t) \approx -iat - (b/2)t^2$, where coefficients a and b are defined as $a = \int_{\tau_e^{-1}}^{\infty}(1 + N_\omega^{(\rm out)} - N_\omega^{(\rm in)})\rho(\omega)d\omega$ and $b = \int_{\tau_e^{-1}}^{\infty}\omega\rho(\omega)B_\omega d\omega$. Using this expansion for $J(t)$, we obtain the following result for the density function $P(\omega)$:

$$P(\varepsilon) = (1/\sqrt{2\pi b})\exp[-(\varepsilon - a)^2/2b]. \tag{7}$$

Here the expansion parameter a can be estimated as $a = a_0(1 + \frac{(T_e - T_{\rm env})\ln(\omega_{\rm max}\tau_e)}{\pi\omega_{\rm max}})$, where $a_0 = 2\int\rho d\omega \approx 2\rho(0)\omega_{\rm max} \approx 2E_c$, where E_c is the charging energy of the tunnel junction, T_e is the electron temperature in the junction, $T_{\rm env}$ is the temperature of environmental modes, and $\omega_{\rm max} \approx 1/(R_TC)$. Similarly to coefficient b in Eq. (7), we obtain $b \approx a_0(T_e + T_{\rm env})$.

Substituting the density $P(\omega)$, Eq. (7), into the heat flux $\dot{Q}$, Eq. (1), we obtain our first main result for the typical heat exchange of the ohmic environment with the tunnel junction between two normal leads. The full temperature and voltage dependence is shown in Fig. 3.

V. DYNAMIC COULOMB INTERACTION

Next we discuss the more realistic situation where the tunneling junction is connected to two disordered conductors (leads). Following Ref. 9, one can find the spectral probability function $\rho(\omega)$ corresponding to the electron-environment interaction,

$$\rho_{\rm ij}(\omega) = \frac{\omega}{2\pi}Im\sum_{\mathbf{q}}\frac{\left(\frac{2\pi}{L}\right)^2(2\delta_{\rm ij} - 1)\tilde{U}_{\rm ij}(\mathbf{q},\omega)}{(\mathcal{D}_i q^2 - i\omega)(\mathcal{D}_j q^2 - i\omega)}, \tag{8}$$

where $i, j = 1,2$ are the lead indices, $\mathcal{D}_{1(2)}$ are diffusion coefficients within the respective electrodes, and $\tilde{U}_{\rm ij}(\mathbf{q},\omega)$ are the dynamically screened Coulomb interactions within (across) the electrodes. The form of spectral probability $\rho(\omega)$ [$\rho(\omega) = 2\rho_{12} + \rho_{11} + \rho_{22}$] depends on the structure of the environmental excitations spectrum and, thus, on the external bias.

The system under consideration is shown in Fig. 4(a): two contacts are separated by distance d and their thickness is a. The external bias is V and the contacts are kept at temperature T and the environment at temperature $T_{\rm env}$.

The screened Coulomb interaction in Eq. (8) in Fourier space has the form $\underline{\tilde{U}}(\mathbf{q},\omega) = \{[\underline{U}^{(0)}(\mathbf{q},\omega)]^{-1} + \underline{\mathcal{P}}(\mathbf{q},\omega)\}^{-1}$, where $\underline{U}^{(0)}(\mathbf{q},\omega) = u(q)\underline{I} + v(q)\underline{\sigma}_x$ is the bare Coulomb interaction and $\underline{\mathcal{P}}(\mathbf{q},\omega)$ the polarization matrix, respectively, with $\mathcal{P}_{\rm ij} = \nu_i\mathcal{D}_i q^2(\mathcal{D}_i q^2 - \imath\omega)^{-1}\delta_{\rm ij}$. ν_i is the electron density of states at the Fermi surface in lead i.

Below we concentrate on quasi-two-dimensional (2D) infinite leads. For this geometry with $a \ll L$, where L is the characteristic lead size in the x and y directions, the bare Coulomb interaction has the form

$$U_{ij}^{(0)}(\mathbf{r}_i - \mathbf{r}_j) = e^2\int dz_i\, dz_j\,\frac{\delta\left(z_i - z_i^{(0)}\right)\delta\left(z_j - z_j^{(0)}\right)}{|\mathbf{r}_i - \mathbf{r}_j|}, \tag{9}$$

with $z_i^{(0)} = (1/2 - \delta_{i1})d$, leading to $u(q) = 2\pi e^2/q$ and $v(q) = 2\pi e^2 e^{-qd}/q$.

In the following, we consider the case of identical leads with the same diffusion coefficients $\mathcal{D}_1 = \mathcal{D}_2 \equiv \mathcal{D}$ and densities of states, $\nu_1 = \nu_2 \equiv \nu$. The dimensionless matrix elements $\tilde{U}_{ij}$ of the dynamically screened Coulomb interaction (in units of e^2d) are then given by

$$\tilde{U}_{\rm ii} = \frac{4\pi}{\tilde{q}}\frac{\chi(\tilde{q})}{\chi^2(\tilde{q}) - \coth^{-2}(\tilde{q})}, \quad \tilde{U}_{\rm i\neq j} = \frac{\tilde{U}_{ii}}{\chi(\tilde{q})\coth(\tilde{q})}, \tag{10}$$

where $\tilde{q} = dq$ and $\tilde{\omega} \equiv \omega(d^2/\mathcal{D})$, with the dimensionless function $\chi(\tilde{q}) \equiv 1 + \coth(\tilde{q}) + \frac{4\pi e^2 d\nu x}{\tilde{q}^2 - i\tilde{\omega}}$. Using these expressions, we can write Eq. (8) as

$$\rho(\tilde{\omega}) = \frac{2e^2 d}{\mathcal{D}}\tilde{\omega} Im \int_0^\infty \tilde{q} d\tilde{q} \frac{\tilde{U}_{11}[1 - (\chi(\tilde{q})\coth(\tilde{q}))^{-1}]}{(\tilde{q}^2 - i\tilde{\omega})^2}.$$

Using this expression we can calculate the heat flux $\dot{Q}$ in Eq. (1) between environment and nanojunction with dynamic Coulomb interaction. The typical energy scale is given by the Thouless energy for a junction of distance d, $E_{\rm th} = \mathcal{D}/d^2$, which we use to rewrite all expressions in dimensionless units. For a typical temperature $E_{\rm th} \approx 100$ K, the temperature and voltage dependence is numerically calculated and shown in Fig. 4(b). Again, the nonequilibrium heat flow $\dot{Q}$ is up to an order of magnitude larger than the quasiequilibrium approximation $\dot{Q}_0$. We remark that, in this case, the function $\rho(\omega)$ introduces a natural cutoff for $J(t)$ which behaves as $\sim -|t|$ for large t.

VI. DISCUSSION

Above, we have assumed that the density of hot electrons is high enough so that the electron-electron scattering time is smaller than the time of energy relaxation (this time is large because of the quasielastic nature of interaction between the electrons and the environment). In this case the electron distribution function is close to an equilibrium one with an electron temperature T_e, which, in the high-voltage limit, is higher than the environment temperature $T_{\rm env}$.

In summary, we have discussed the influence of far-from-equilibrium heating effects on properties of nanojunctions. Based on a quantum-kinetic approach, we calculated the nonlinear heat flux between environment and junction. We showed that the resulting freezing or heating effects far from equilibrium are, by orders of magnitude, larger than estimates based on quasiequilibrium environment theory. We obtained analytical results for the heat flow in an idealized high-impedance environment and demonstrated, numerically, that these results hold for the more general case of an environment with Coulomb interaction. We showed that the environment can be a very effective freezing agent if the effective temperature well exceeds the high-frequency cutoff $\hbar\omega_{\rm max}$. From the experimental point of view the temperature regime in which the effect is present is readily accessible. However, one needs to measure the time dependence of the junction temperature in order to extract $\dot{Q}$, which could be technically challenging for a nanojunction, and the presence of a substrate might need consideration.

One can expect that our results, in particular, the giant freezing effect, will be important for electronic transport in junction arrays,[10] which will be the subject of a forthcoming work.

ACKNOWLEDGMENTS

We are grateful to J. Pekola and F. Hekking for useful discussions. This work was supported by the US Department of Energy Office of Science under Contract No. DE-AC02-06CH11357. I.B. was supported by an award from the Research Corporation for Science Advancement and the Materials Theory Institute at ANL.

APPENDIX A: HEAT FLOW RATE

In this appendix we present a derivation of Eq. (1) for the rate of the heat flow. A general formula for the heat current going from the left electrode (1) toward the right electrode reads

$$I_q^{1\to} = -\left(\Gamma_q^{1,\rm in} - \Gamma_q^{1,\rm out}\right), \tag{A1}$$

where $\Gamma_q^{1\to}$ ($\Gamma_q^{1\leftarrow}$) is the heat transfer tunneling rate calculated in the left electrode:

$$\Gamma_q^{1,\rm out} = \frac{1}{R_T}\int_{\epsilon\epsilon'}(\epsilon - \phi_1) f_\epsilon^{(1)}\left(1 - f_{\epsilon'}^{(2)}\right) P(\epsilon - \epsilon'),$$
$$\Gamma_q^{1,\rm in} = \frac{1}{R_T}\int_{\epsilon\epsilon'}(\epsilon' - \phi_1)\left(1 - f_{\epsilon'}^{(1)}\right) f_\epsilon^{(2)} P(\epsilon - \epsilon').$$

Under the gauge transformation $\phi \to \phi - \partial_t k$, the distribution functions transform like $f^{(i)}(\epsilon) \to f^{(i)}(\epsilon + \partial_t k)$. Therefore the rates and the heat current defined above are gauge invariant.

Similarly, we can find

$$I_q^{2\to} = -\left(\Gamma_q^{2,\rm out} - \Gamma_q^{2,\rm in}\right), \tag{A2}$$

where $\Gamma_q^{2\to}$ ($\Gamma_q^{2\leftarrow}$) is the heat transfer tunneling rate calculated in the right electrode:

$$\Gamma_q^{2,\rm out} = \frac{1}{R_T}\int_{\epsilon\epsilon'}(\epsilon - \phi_2) f_\epsilon^{(2)}\left(1 - f_{\epsilon'}^{(1)}\right) P(\epsilon - \epsilon'),$$
$$\Gamma_q^{2,\rm in} = \frac{1}{R_T}\int_{\epsilon\epsilon'}(\epsilon' - \phi_2)\left(1 - f_{\epsilon'}^{(2)}\right) f_\epsilon^{(1)} P(\epsilon - \epsilon').$$

The gradient of the heat current, ∇I_Q, at the contact is

$$\nabla I_Q = I_q^{2\to} - I_q^{1\to} = \left\{\Gamma_q^{1,\rm out} - \Gamma_q^{2,\rm in}\right\} + \left\{\Gamma_q^{2,\rm out} - \Gamma_q^{1,\rm in}\right\}.$$

Finally, we find

$$\nabla I_Q = (\phi_2 - \phi_1) I + \frac{1}{R_T}\int_{\epsilon\epsilon'}(\epsilon - \epsilon') P(\epsilon - \epsilon') \times \left\{f_\epsilon^{(1)}\left(1 - f_{\epsilon'}^{(2)}\right) + f_\epsilon^{(2)}\left(1 - f_{\epsilon'}^{(1)}\right)\right\}.$$

On the other hand, the conservation law demands

$$\dot{Q} + \nabla I_Q = \mathcal{E} I, \tag{A3}$$

where the right-hand side is the Joule heat, which is related to the work of the electric field. The Joule heat is dissipated in the bulk of the electrodes at distance l_E from the junction, where l_E is the energy relaxation length. The heat $\dot{Q}$ is the heat dissipated into the environment:

$$\dot{Q} = \frac{1}{R_T}\int_{\epsilon\epsilon'}(\epsilon - \epsilon') \sum_{i,j} f_\epsilon^{(i)} \sigma_{ij}^x \left(1 - f_{\epsilon'}^{(j)}\right) P(\epsilon - \epsilon'), \tag{A4}$$

where σ_x is the Pauli matrix. Equation (A4) can be rewritten in terms of "Bose" distribution functions as follows:

$$\dot{Q} = \int_0^\infty d\varepsilon\, \varepsilon p(\varepsilon)\{n_\varepsilon P^<(\varepsilon) - [1 + n_\varepsilon] P(-\varepsilon)\}, \tag{A5}$$

with $p(\varepsilon) = 4\varepsilon/R_T$ and $n_\varepsilon = \{(\varepsilon - V)N_B(\varepsilon - V, T) + (\varepsilon + V)N_B(\varepsilon + V, T)\}/2\varepsilon$. Equation (A5) coincides with Eq. (1) in

the text. In the zero-voltage limit, Eq. (A5) agrees with the corresponding expression in Ref. 5.

APPENDIX B: HEAT FLOW AT SECOND ORDER IN $\rho(\varepsilon)$

Below Eq. (3), Dbwe derived the heat flow $\dot{Q}$ in the leading (first) order in spectral function $\rho(\varepsilon)$. In this appendix we show that the heat flow $\dot{Q}$ at second order in the electron-environment interaction and at first (leading) order in the temperature difference $\delta T = T_e - T_{\rm env}$ leads to the same enhancement as the first order term.

The heat flow can be written as a sum of two terms, $\dot{Q} = (W_1 + W_2)\tau$, where

$$W_1 = \frac{1}{2}\int_{-\infty}^{\infty} d\varepsilon\, \varepsilon p(\varepsilon)[\partial_{\tilde{T}} n_\varepsilon] P(\varepsilon), \tag{B1}$$

$$W_2 = \int_0^{\infty} d\varepsilon\, \varepsilon p(\varepsilon) n_\varepsilon \partial_\tau \{P(\varepsilon) - P(-\varepsilon)\}. \tag{B2}$$

Here $\tilde{T} = (T_e + T_{\rm env})/2$. Typically, $W_1 \lesssim W_2$; therefore we concentrate on contribution W_2 below.

At second order in electron-environment interaction [function $\rho(\varepsilon)$], we obtain the following result for the heat flow:

$$\begin{aligned}\dot{Q}^{(2)} \propto \int_0^{\infty} d\varepsilon d\varepsilon_1 d\varepsilon_2 \varepsilon p(\varepsilon) \frac{\rho(\varepsilon_1)}{\varepsilon_1}\frac{\rho(\varepsilon_2)}{\varepsilon_2}\Big\{ & n_\varepsilon^{(12)}\big(1 + N_{\varepsilon_1}^{(\rm out)}\big) \\ & \times \big(1 + N_{\varepsilon_2}^{(\rm out)}\big)\delta_{\varepsilon-\varepsilon_1-\varepsilon_2} + n_\varepsilon^{(12)} N_{\varepsilon_1}^{(\rm in)}\big(1 + N_{\varepsilon_2}^{(\rm out)}\big)\delta_{\varepsilon+\varepsilon_1-\varepsilon_2} \\ & + n_\varepsilon^{(12)}\big(1 + N_{\varepsilon_1}^{(\rm out)}\big) N_{\varepsilon_2}^{(\rm in)}\delta_{\varepsilon-\varepsilon_1+\varepsilon_2} - \big(1 + n_\varepsilon^{(12)}\big) \\ & \times N_{\varepsilon_1}^{(\rm in)} N_{\varepsilon_2}^{(\rm in)}\delta_{\varepsilon-\varepsilon_1-\varepsilon_2} - \big(1 + n_\varepsilon^{(12)}\big)\big(1 + N_{\varepsilon_1}^{(\rm out)}\big) \\ & \times N_{\varepsilon_2}^{(\rm in)}\delta_{\varepsilon+\varepsilon_1-\varepsilon_2} - \big(1 + n_\varepsilon^{(12)}\big) N_{\varepsilon_1}^{(\rm in)}\big(1 + N_{\varepsilon_2}^{(\rm out)}\big)\delta_{\varepsilon-\varepsilon_1+\varepsilon_2}\Big\}. \end{aligned} \tag{B3}$$

At low frequencies ($T \gg \varepsilon$) we find the W_2 contribution to $\dot{Q}^{(2)}$ as follows:

$$\begin{aligned} & n_\varepsilon^{(12)}\big(1 + N_{\varepsilon_1}^{(\rm out)}\big)\big(1 + N_{\varepsilon_2}^{(\rm out)}\big) - \big(1 + n_\varepsilon^{(12)}\big) N_{\varepsilon_1}^{(\rm in)} N_{\varepsilon_2}^{(\rm in)} \\ & \quad \approx n_\varepsilon^{(12)}\frac{(T_e)^2}{\varepsilon_1\varepsilon_2} - \big(1 + n_\varepsilon^{(12)}\big)\frac{(T_{\rm env})^2}{\varepsilon_1\varepsilon_2} \\ & \quad \approx \cdots + (T_e - T_{\rm env})\big(1 + 2n_\varepsilon^{(12)}\big)\frac{T_e + T_{\rm env}}{2\varepsilon_1\varepsilon_2} + \cdots. \end{aligned} \tag{B4}$$

Here dots represent the terms that finally cancel in Eq. (B3). We mention the presence of a large enhancement factor $(1 + 2n_\varepsilon^{(12)}) \approx (T_e + T_{\rm env})/\varepsilon \gg 1$ in Eq. (B4).

In the quasiequilibrium case we do not have this large factor. Indeed, in this case we have

$$\begin{aligned} & n_\varepsilon^{(12)}\big(1 + N_{\varepsilon_1}^{(\rm out)}\big)\big(1 + N_{\varepsilon_2}^{(\rm out)}\big) - \big(1 + n_\varepsilon^{(12)}\big) N_{\varepsilon_1}^{(\rm in)} N_{\varepsilon_2}^{(\rm in)} \\ & \quad \approx n_\varepsilon^{(12)}\frac{(T_e)^2}{\varepsilon_1\varepsilon_2} - \big(1 + n_\varepsilon^{(12)}\big)\frac{(T_e)^2}{\varepsilon_1\varepsilon_2} \\ & \quad \approx \cdots + (T_e - T_{\rm env})\frac{T_e + T_{\rm env}}{2\varepsilon_1\varepsilon_2} + \cdots. \end{aligned} \tag{B5}$$

To conclude, at second order in function $\rho(\varepsilon)$, the heat flow $\dot{Q}$ is enhanced by the same factor $(T_e + T_{\rm env})/\varepsilon \gg 1$ as at first order. Similar results can be proofed at higher orders in $\rho(\varepsilon)$.

*n.chtchelkatchev@gmail.com

[1] A. F. Volkov and S. M. Kogan, Usp. Fiz. Nauk **96**, 633 (1968); Sov. Phys. Usp. **11**, 881 (1969); A. V. Gurevich and R. G. Mints, Rev. Mod. Phys. **59**, 941 (1987).

[2] F. Giazotto, T. T. Heikkilä, A. Luukanen, A. M. Savin, and J. P. Pekola, Rev. Mod. Phys. **78**, 217 (2006).

[3] N. M. Chtchelkatchev, V. M. Vinokur, and T. I. Baturina, Phys. Rev. Lett. **103**, 247003 (2009).

[4] Since the current-voltage characteristic $I(V)$ becomes linear only at high voltages, R_T is defined at large V.

[5] D. R. Schmidt, R. J. Schoelkopf, and A. N. Cleland, Phys. Rev. Lett. **93**, 045901 (2004); M. Meschke, W. Guichard, and J. P. Pekola, Nature (London) **444**, 187 (2006).

[6] H. Grabert and M. H. Devoret, in *Single Charge Tunneling*, *NATO ASI, Series B*, edited by H. Grabert and M. H. Devoret (Plenum, New York, 1991), Vol. 294, p. 1.

[7] J. P. Pekola and F. W. J. Hekking, Phys. Rev. Lett. **98**, 210604 (2007); D. V. Anghel and J. P. Pekola, J. Low Temp. Phys. **123**, 197 (2001).

[8] Ya. M. Blanter, M. Büttiker, Phys. Rep. **336**, 1 (2000).

[9] J. Rollbühler and H. Grabert, Phys. Rev. Lett. **87**, 126804 (2001).

[10] A. Glatz and I. S. Beloborodov, Phys. Rev. B **81**, 033408 (2010); A. Glatz, I. S. Beloborodov, N. M. Chtchelkatchev, and V. M. Vinokur, *ibid.* **82**, 075314 (2010).